Electronic Supplementary Material (ESI) for Journal of Materials Chemistry A.

Supporting Information

Efficient methane oxidation to oxygenates over etched ZnCr layered double hydroxide nanosheets

*Lei Wu,‡ Dandan Liu,‡ Fan Chen, Huanyu Zhou, Rui Shi, Yana Liu, Jiguang Zhang, Yunfeng Zhu and Jun Wang**

College of Materials Science and Engineering, Jiangsu Collaborative Innovation Centre for Advanced Inorganic Function Composites, Nanjing Tech University, 30 South Puzhu Road, Nanjing, 211816, P. R. China

1. Experimental section

1.1. Materials

All reagents were used as received. Zinc nitrate hexahydrate ($Zn(NO_3)_2 \cdot 6H_2O$), chromium(III) oxide (Cr_2O_3) and 30% hydrogen peroxide aqueous solution (H_2O_2) were purchased from Sinopharm Chemical Reagent Co., Ltd. Chromium(III) nitrate nonahydrate ($Cr(NO_3)_3 \cdot 9H_2O$), sodium chromate tetrahydrate ($Na_2CrO_4 \cdot 4H_2O$), chromium(VI) oxide (CrO_3), sodium hydroxide (NaOH), sodium carbonate (Na_2CO_3), acetylacetone ($C_5H_8O_2$), 5,5-Dimethyl-1-pyrroline N-oxide ($C_6H_{11}NO$), zinc acetate dihydrate ($C_4H_6O_4Zn \cdot 2H_2O$), oxalic acid ($C_2H_2O_4$), deuterium oxide (D_2O, 99.9% D) and 1,4-dioxane ($C_4H_8O_2$) were bought from Shanghai Aladdin Bio-Chem. Technology Co., Ltd. CH_4 (99.999%) and Ar (99.999%) were obtained from the Nanjing Shangyuan Gas. The deionized water was utilized in all experiments, which has a resistivity of 18.2 MΩ·cm.

1.2. Synthesis of ZnCr-LDH nanosheets

For a typical experiment, 0.04 mol $Zn(NO_3)_2 \cdot 6H_2O$ and 0.02 mol $Cr(NO_3)_3 \cdot 9H_2O$ were first dissolved in 30 mL of deionized water. Then, 40 mL of aqueous solution containing 0.12 mol NaOH and 0.1 mol Na_2CO_3 were added dropwise into the above solution under constant stirring. The slurry was further heated at 60 ^oC in an oil bath for 24 h. Subsequently, the precipitates were collected by centrifugation and washed with deionized water for five times. Finally, the as-prepared ZnCr-LDH nanosheets were freeze-dried overnight.

1.3. Alkali etching of ZnCr-LDH nanosheets

First, 300 mg of ZnCr-LDH nanosheets was dispersed in 20 mL of deionized water and sonicated for 30 min. Then the suspension was mixed with 60 mL of aqueous solution containing 0.06 mol NaOH. After stirring for 10 minutes, the mixture was transferred to a Teflon-lined

autoclave and heated at 120 °C for various times. After cooling to room temperature, the product was collected by centrifugation and washed with deionized water for five times. Finally, the product was freeze-dried overnight to obtain etched ZnCr-LDH nanosheets.

1.4. Synthesis of ZnO nanoparticles

1.487 g of $Zn(NO_3)_2 \cdot 6H_2O$ and 0.45 g of oxalic acid were dissolved in 100 mL of deionized water, respectively. The oxalic acid solution was then added into metal precursor solution to obtain the precipitates. Subsequently, the precipitates were filtered, washed with deionized water, and freeze-dried overnight. Finally, the solid powder was calcined at 350 °C in air for 6 h to obtain ZnO nanoparticles.

1.5. Material characterization

The crystal structures and crystallinity of the samples were analyzed by X-ray diffraction (XRD) with Cu Kα radiation (40 kV and 35 mA) using an ARL-X'TRA diffractometer. Transmission electron microscopy (TEM) images were carried out using JEM-2010 electron microscope. High-angle annular dark-field scanning transmission electron microscopy (HAADF-STEM) images, SAED and elemental mapping were performed using FEI Talos F200X G2 electron microscope. The field emission scanning electron microscopy (FE-SEM) images were performed to detect the morphology of the samples by using JSM-5900. X-ray photoelectron spectroscopy (XPS) was recorded in Thermo Scientific K-Alpha. The Zn^{2+}/Cr^{3+} molar ratios of ZnCr-LDH nanosheets were measured by inductively coupled plasma-optical emission spectrometry (ICP-OES, PerkinElmer Avio200). Brunauer-Emmett-Teller (BET) surface areas were collected by Nitrogen adsorption-desorption isotherms using Micromeritics ASAP 2460 at 77 K. Fourier transform infrared (FT-IR) spectra was carried out in a range of 4000-500 cm^{-1} by Thermo Scientific Nicolet iS5. Raman spectra were recorded on LabRAM HR Evolution with a

diode laser emitting 532 nm. Low-temperature electron paramagnetic resonance (EPR) spectroscopy measurement was performed on Bruker EMX plus at 77 K to detect vacancies.

1.6. Detection of reactive radicals

The reactive radicals were detected by EPR measurements at room temperature using a Bruker A200 EPR spectrometer, where 5,5-dimethyl-1-pyrroline N-Oxide (DMPO) was used as the trapping agent. Typically, for the detection of ·OH and ·OOH radicals, the sample (10 mg) was dispersed in a mixed solution containing water (5 mL) and H_2O_2 solution (200 μL, 30 wt % in H_2O). Then, 200 μL of the dispersion was mixed with 100 μL of DMPO aqueous solution (300 mM), which was stirred for 1 min to capture the reactive radicals before the EPR measurements.

1.7. Catalytic activity measurements

The methane oxidation reaction with H_2O_2 was carried out in a 220 mL batch-reactor. Typically, 10 mg catalyst was dispersed in 50 mL deionized water by ultrasonication for 20 min. H_2O_2 solution (0-2 mL, 30 wt % in H_2O) was added into the above solution under stirring. After sealing, the batch-reactor was purged with Ar for 15 min to exhaust air and then pressurized with 20 bar methane, which was stirred for 10 more minutes to ensure the dissolution of methane in the reaction solution. Afterwards, the reactor was heated to 50 ^oC with constant stirring at 500 rpm. After 1h of the reaction, the reactor was cooled in an ice-water bath to reduce product volatilization.

1.8. Products analysis and quantification

The liquid oxygenates products (CH_3OH, CH_3OOH, $HOCH_2OOH$, HCOOH) were quantified by nuclear magnetic resonance (Bruker AVANCE III 400 MHz). Typically, 0.5 mL liquid product was mixed with 0.1 mL D_2O containing 0.01% (v/v) 1, 4-Dioxane as the internal standard (Fig. S9). The water suppression technique was applied during the NMR measurements. The gas product

(CO_2) was analyzed by gas chromatograph (GC 9790 PLUS, Zhejiang Fuli Analytical Instrument Co., Ltd) equipped with a thermal conductivity detector (TCD) and a flame ionization detector (FID).

Liquid product HCHO was quantified by the acetylacetone colorimetric method.[1] Typically, 25 g ammonium acetate was dissolved in 50 mL deionized water, then 3 mL acetic acid and 0.25 mL acetylacetone were added. Afterwards, the solution was diluted to 100 mL with deionized water. The obtained 0.25% (v/v) acetylacetone solution was stored at 2-5 ^{o}C before use. After catalytic reaction, 3 mL liquid product solution was mixed with 2 mL 0.25% (v/v) acetylacetone solution. The mixed solution was heated at 100 ^{o}C in an oil bath for 1.5 min, making HCHO react with acetylacetone and ammonia to form yellow-colored 3,5-diacetyl-1,4-dihydrolutidine which can be measured by the absorbance at 413 nm with an ultraviolet-visible (UV-vis) spectrophotometer (TU-1901, Persee Inc.). To quantify the produced HCHO, the calibration curves were built using standard HCHO solutions (Fig. S10).

The H_2O_2 conversion was quantitatively measured by a Ce^{4+} titration method ($2Ce^{4+} + H_2O_2 \rightarrow 2Ce^{3+} + 2H^+ + O_2$).[2] The Ce^{4+} concentration-absorbance curve was plotted by linear fitting the absorbance at 319 nm for various known concentrations of 0, 0.1, 0.2, 0.3, and 0.4 mM of Ce^{4+} (Fig. S12). The sample solutions were mixed with 0.4 mM Ce^{4+} solution by specific dilution, and the absorbance at 319 nm was measured after 10 min. The concentration of H_2O_2 was finally determined based on the reduced Ce^{4+} concentration.

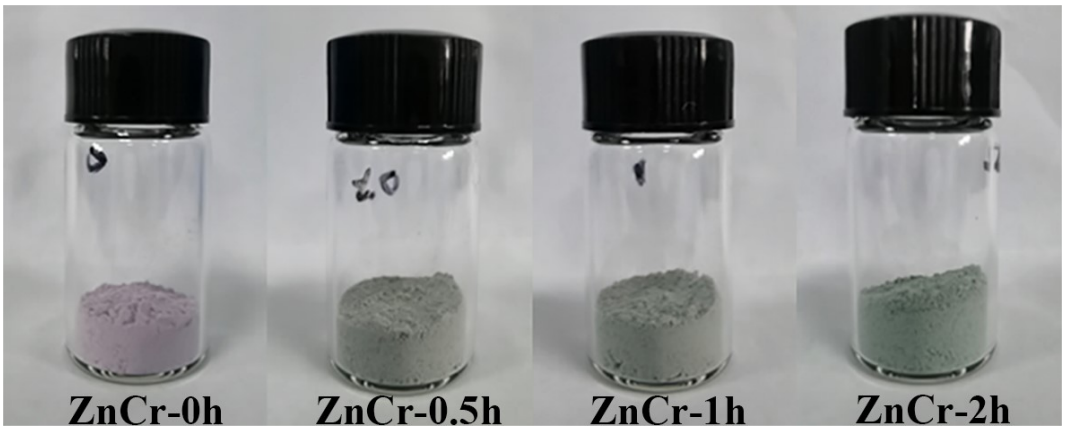

Fig. S1. Digital images of etched ZnCr-xh (x = 0, 0.5, 1 and 2) nanosheets.

Table S1. ICP-OES measurements for ZnCr-xh (x= 0, 0.5, 1, 2) nanosheets.

Sample	Zn/Cr molar ratio		Etched metal content (wt%)		Residual Na content (wt%)
	Nominal	ICP-OES	Zn	Cr	
ZnCr-0h	2:1	2.111:1	/	/	0.094
ZnCr-0.5h	2:1	1.764:1	5.918	0.004	0.087
ZnCr-1h	2:1	1.644:1	7.099	0.013	0.053
ZnCr-2h	2:1	1.478:1	9.544	0.023	0.007

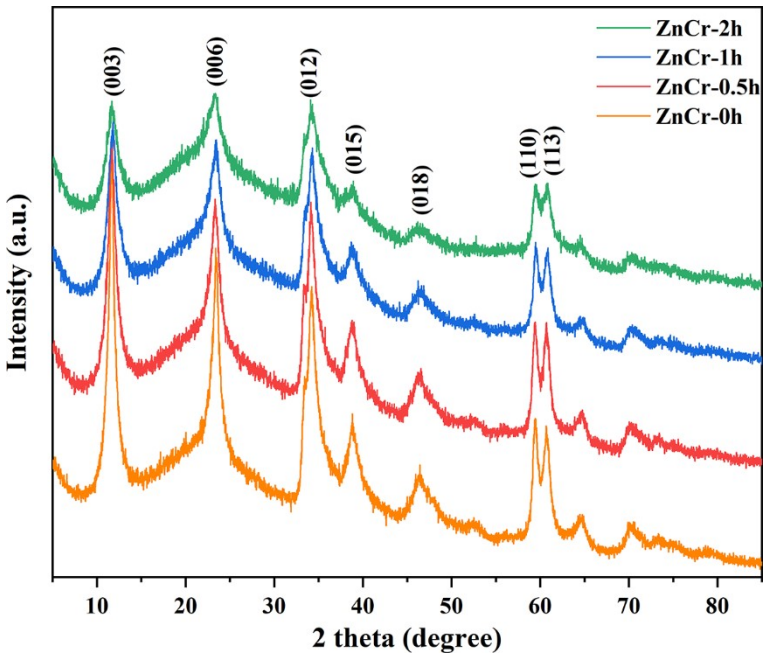

Fig. S2. XRD patterns of etched ZnCr-xh (x = 0, 0.5, 1 and 2) nanosheets.

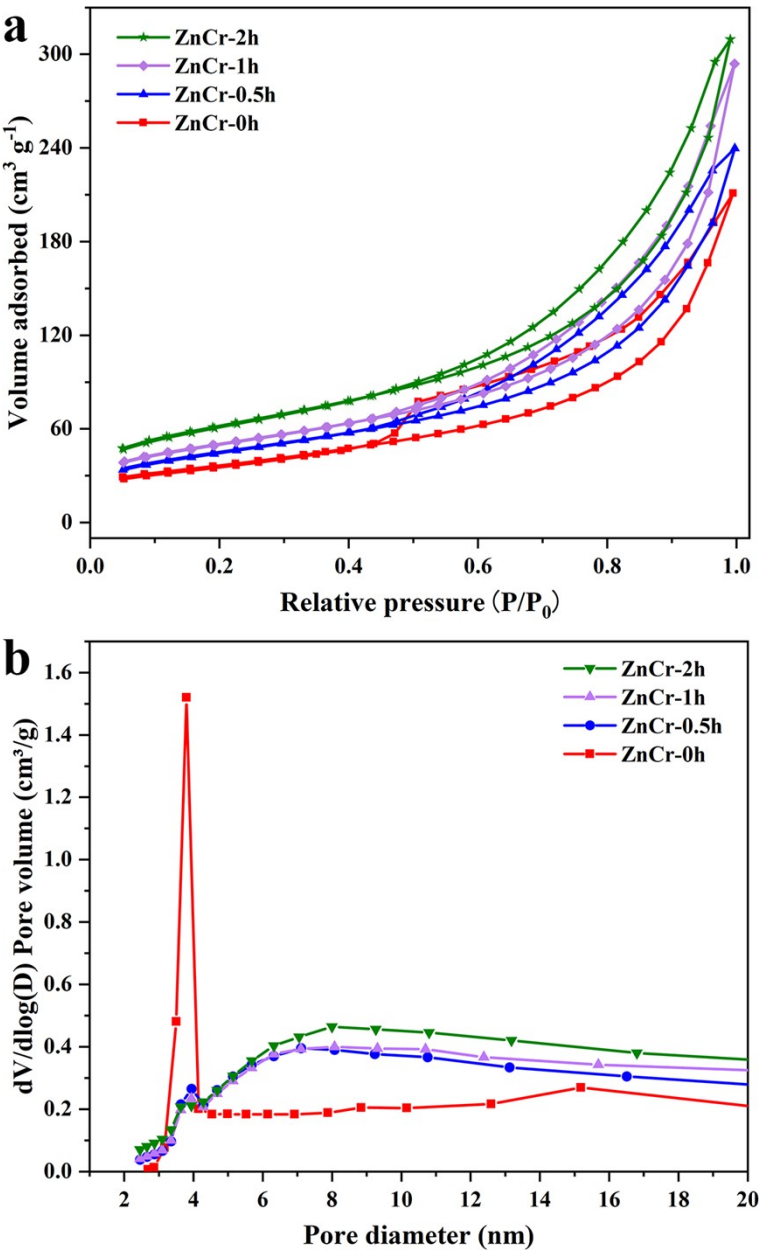

Fig. S3. (a) N_2 adsorption-desorption isotherms and (b) pore size distributions of ZnCr-xh (x = 0, 0.5, 1 and 2) nanosheets.

Table S2. BET surface area of ZnCr-xh (x = 0, 0.5, 1 and 2) nanosheets.

Sample	BET surface area ($m^2 g^{-1}$)
ZnCr-0h	126.1
ZnCr-0.5h	153.1
ZnCr-1h	169.0
ZnCr-2h	207.0

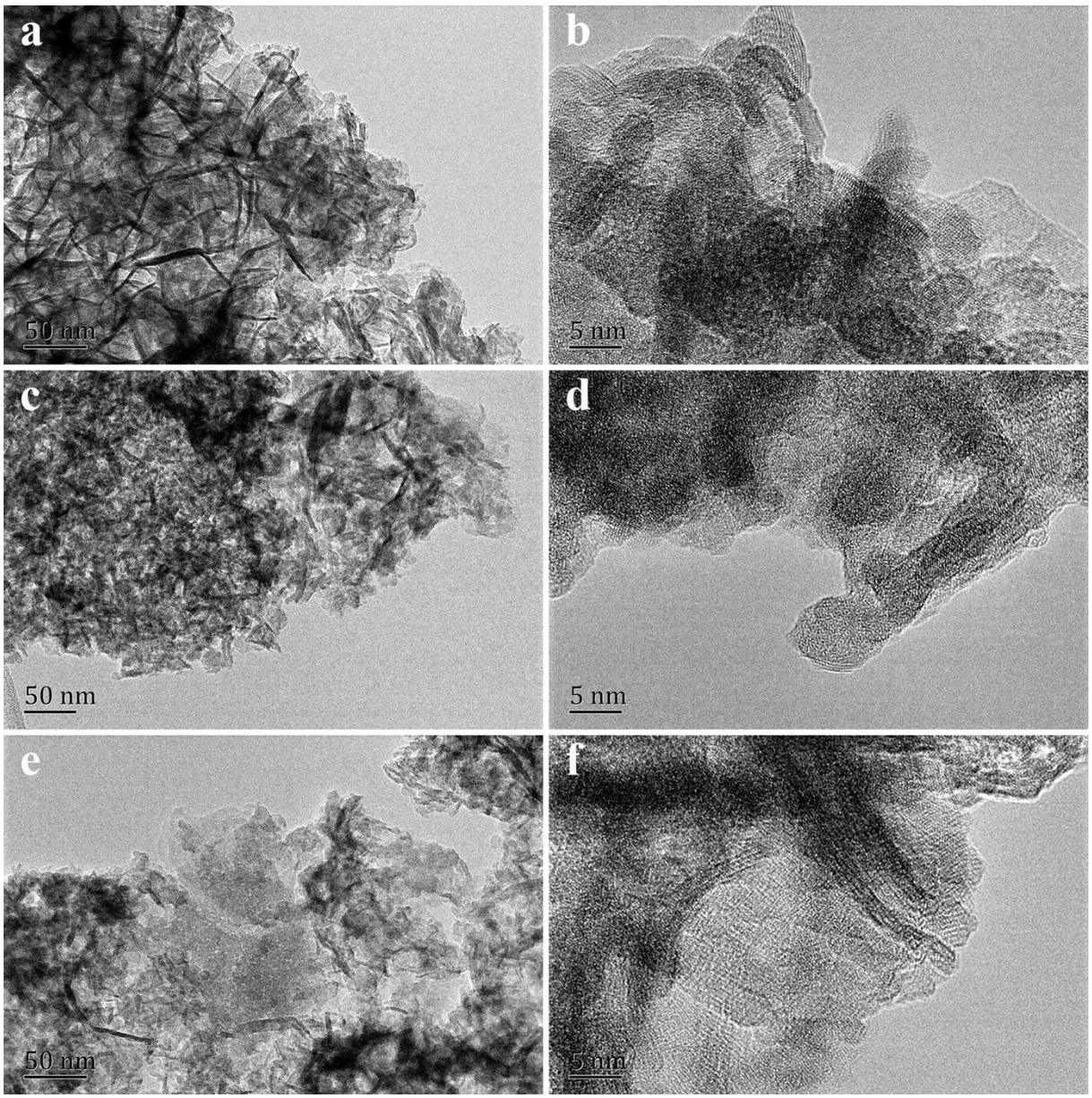

Fig. S4. TEM and HRTEM images of (a-b) ZnCr-0h, (c-d) ZnCr-0.5h, (e-f) ZnCr-2h nanosheets.

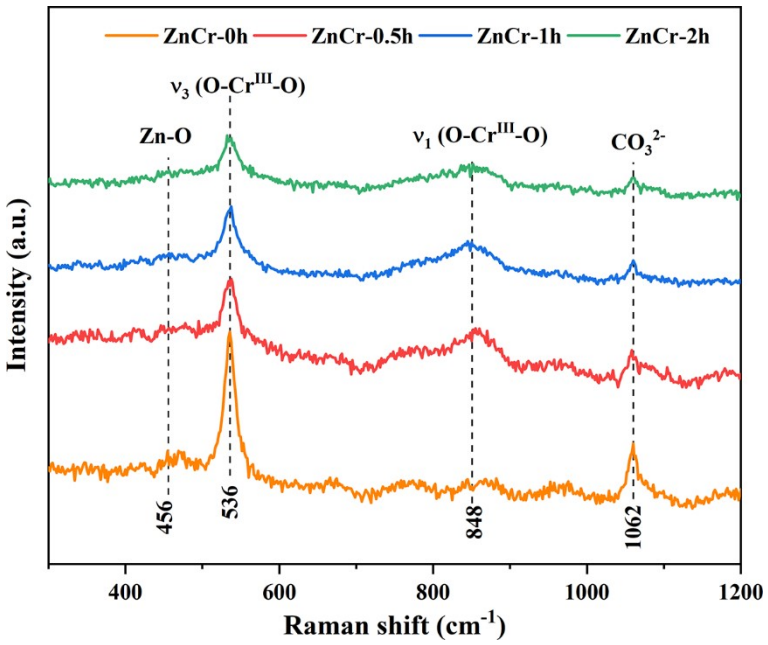

Fig. S5. Raman spectra of ZnCr-xh (x = 0, 0.5, 1 and 2) nanosheets.

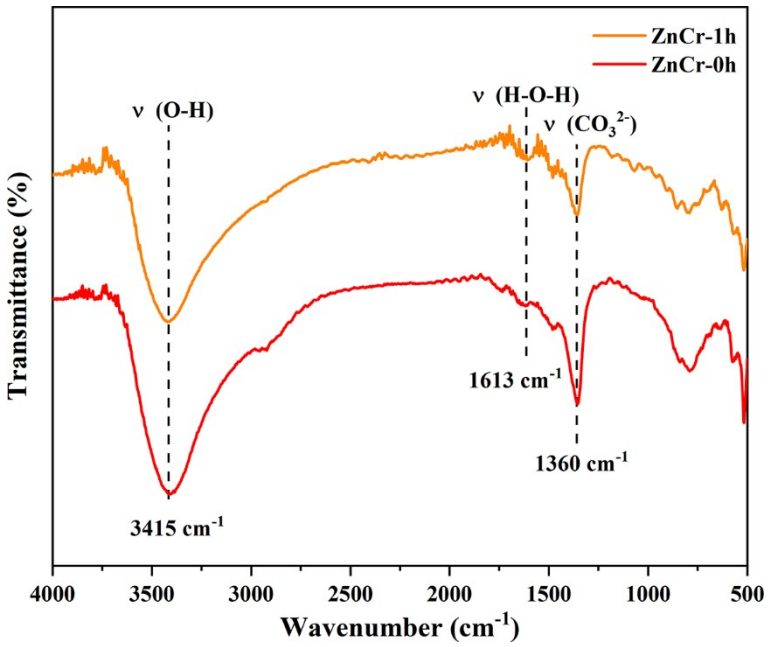

Fig. S6. Fourier-transform infrared spectrum of ZnCr-0h and ZnCr-1h nanosheets.

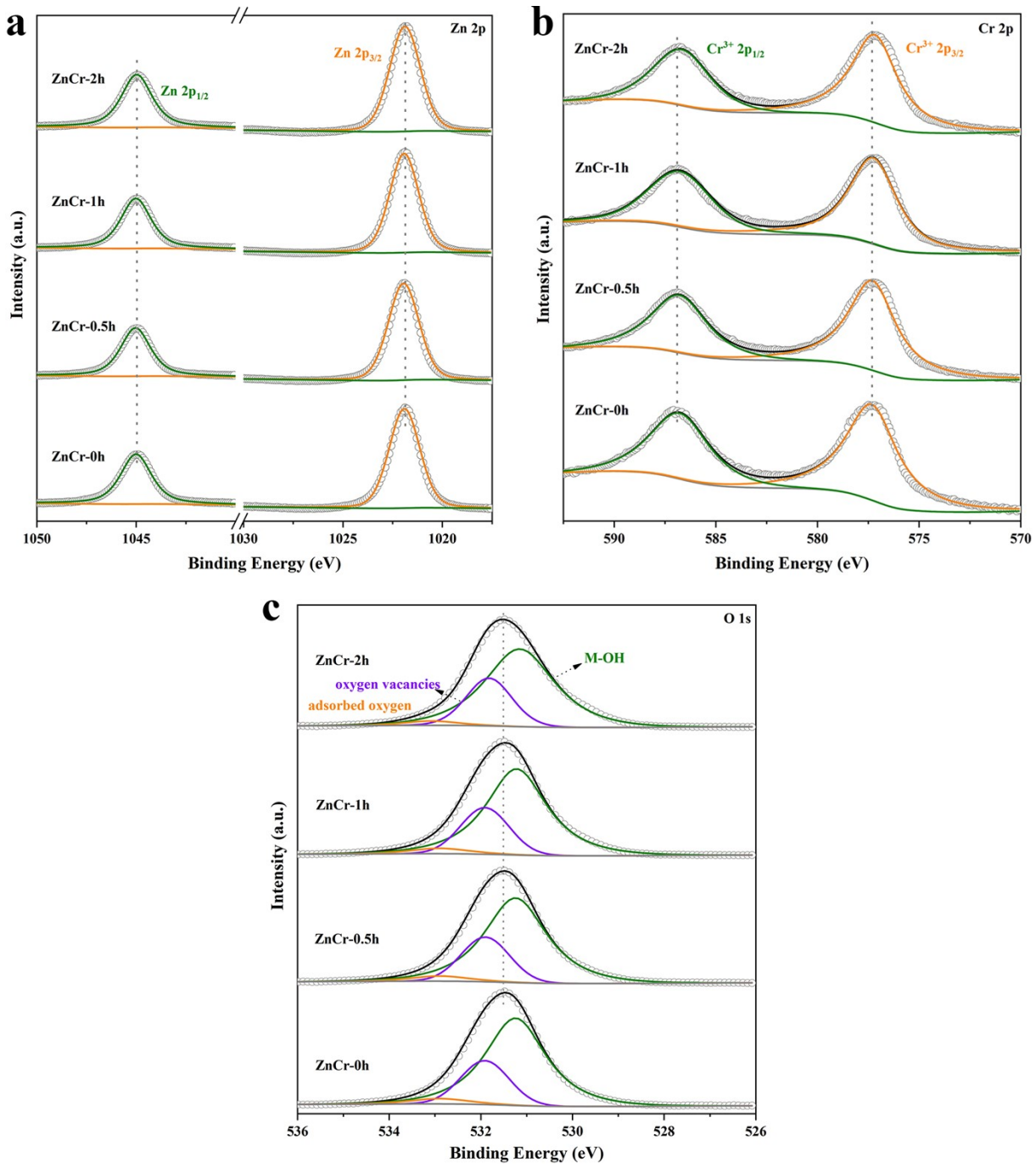

Fig. S7. High-resolution XPS spectra of (a) Zn 2p, (b) Cr 2p and (c) O 1s on ZnCr-xh (x = 0, 0.5, 1 and 2) nanosheets.

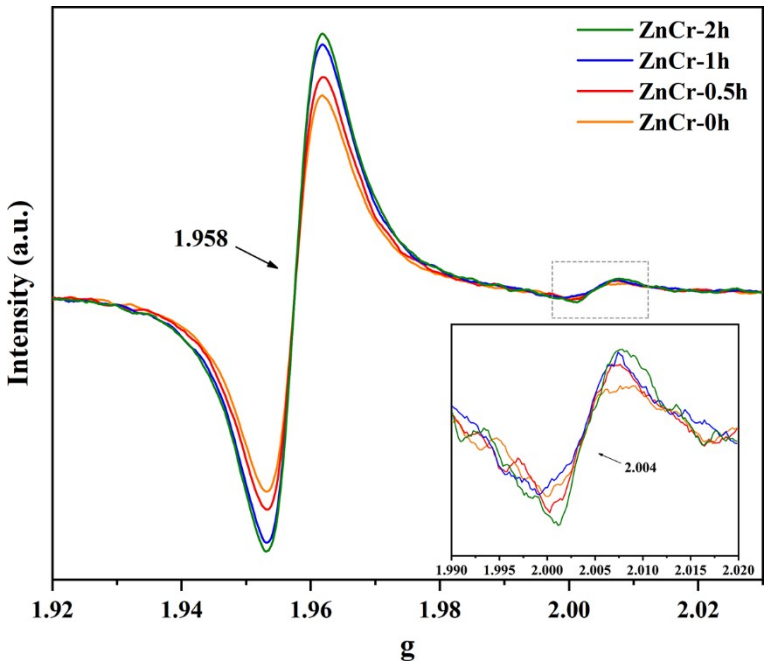

Fig. S8. EPR spectra of ZnCr-xh (x = 0, 0.5, 1 and 2) nanosheets.

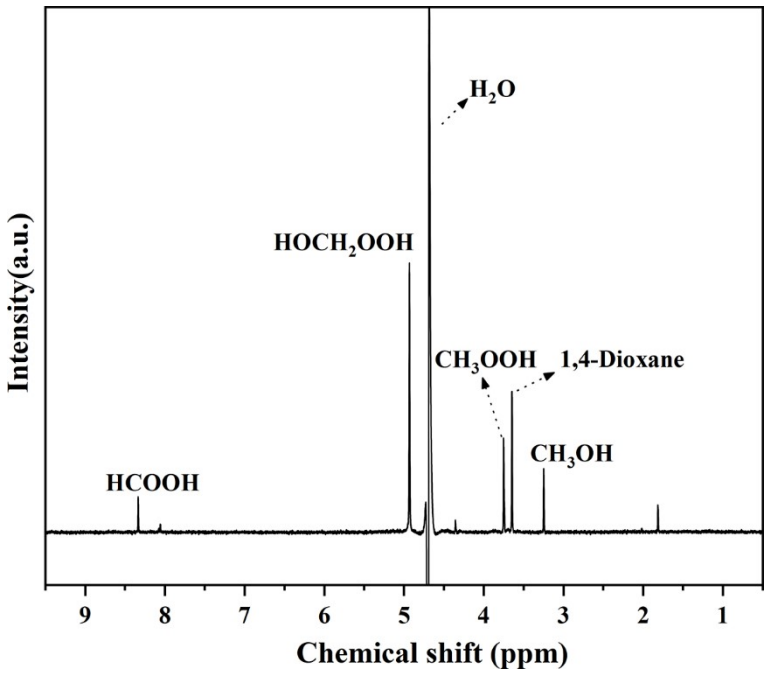

Fig. S9. Typical ^{1}H NMR spectrum of reaction products from CH_4 oxidation over the ZnCr-1h nanosheets for 1 h. Reaction conditions: 10 mg catalyst, 20 bar CH_4, 50 mL H_2O, 1 mL H_2O_2 (30 wt% in H_2O), 1 h reaction time, 50 ^{o}C. The chemical shifts of CH_3OH, CH_3OOH, $HOCH_2OOH$ and HCOOH are located at 3.34, 3.84, 5.02 and 8.43 ppm, respectively. 1,4-dioxane with the chemical shift of 3.74 ppm is used as the internal standard.

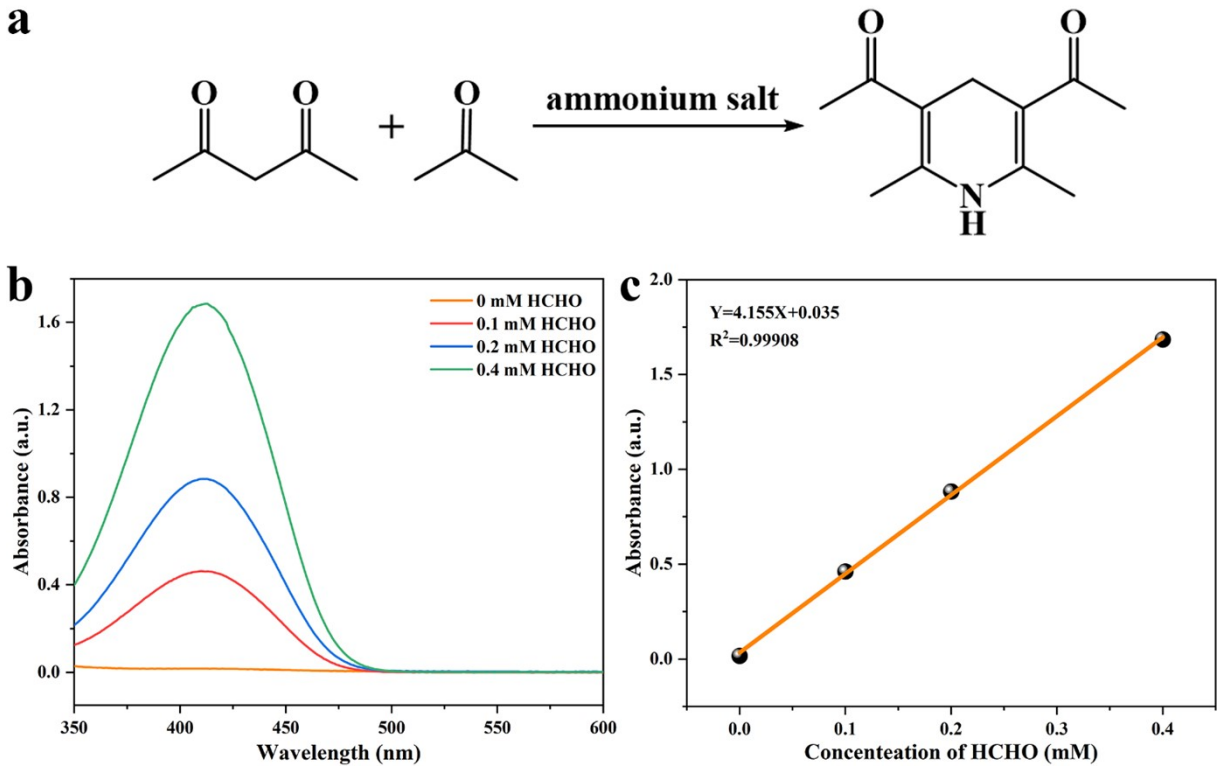

Fig. S10. (a) Reaction mechanism on acetylacetone colorimetric method to detect HCHO. (b) UV-vis absorption spectra of acetylacetone colorimetric method at different HCHO concentration. (c) Calibration curve of HCHO concentration with respect to UV-vis absorption intensity.

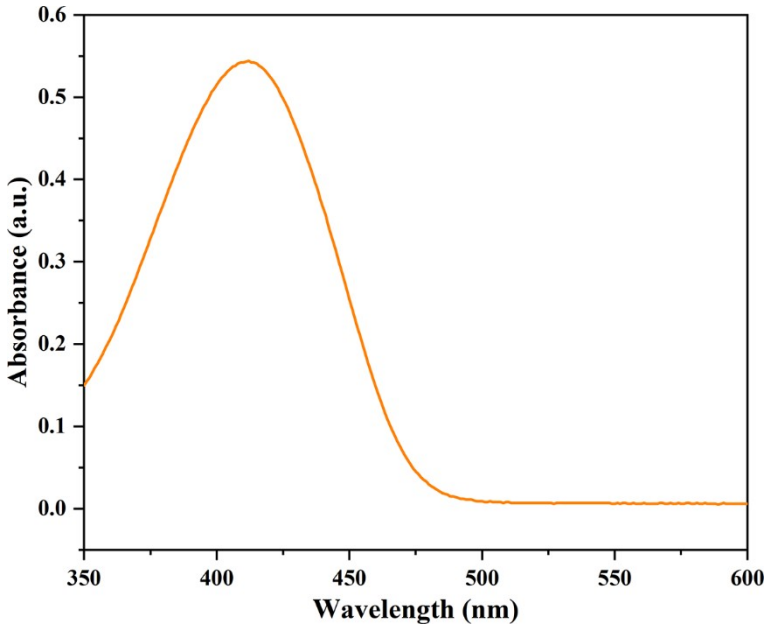

Fig. S11. Typical UV-vis absorption spectrum for quantifying the yield of HCHO over ZnCr-1h with acetylacetone colorimetric method. Reaction conditions: 10 mg catalyst, 20 bar CH_4, 50 mL H_2O, 1 mL H_2O_2 (30 wt% in H_2O), 1 h reaction time, 50 °C.

Since the concentration of the produced HCHO in the solution over ZnCr-1h exceeds the detection limit of the calibration curve in Fig. S10, the presented UV-vis absorption spectrum here is originated from the diluted solution (diluted 15 times with deionized water) after the reaction.

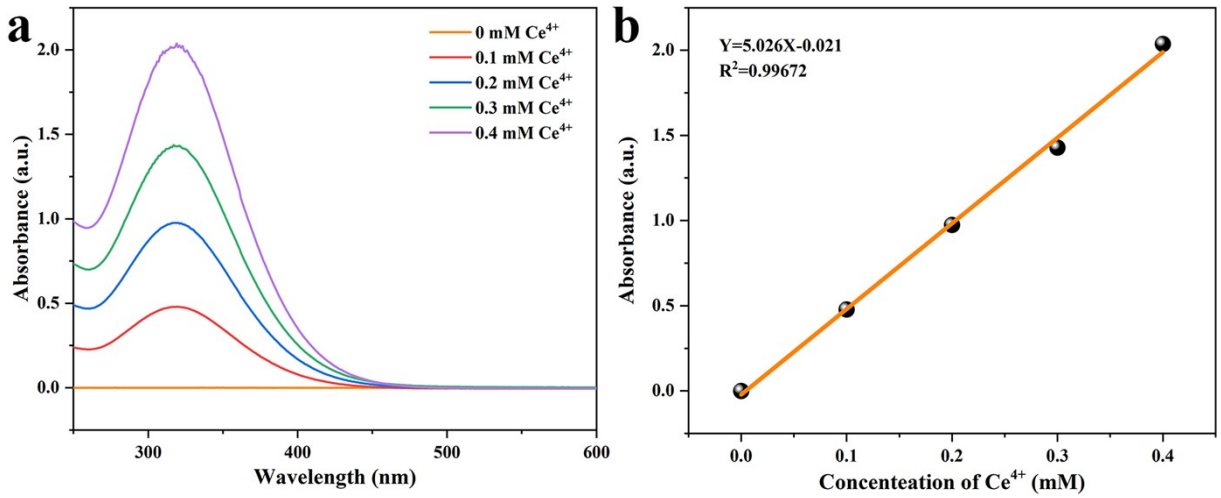

Fig. S12. (a) UV-vis spectra of Ce^{4+} solution with various concentrations and (b) the corresponding calibration curve.

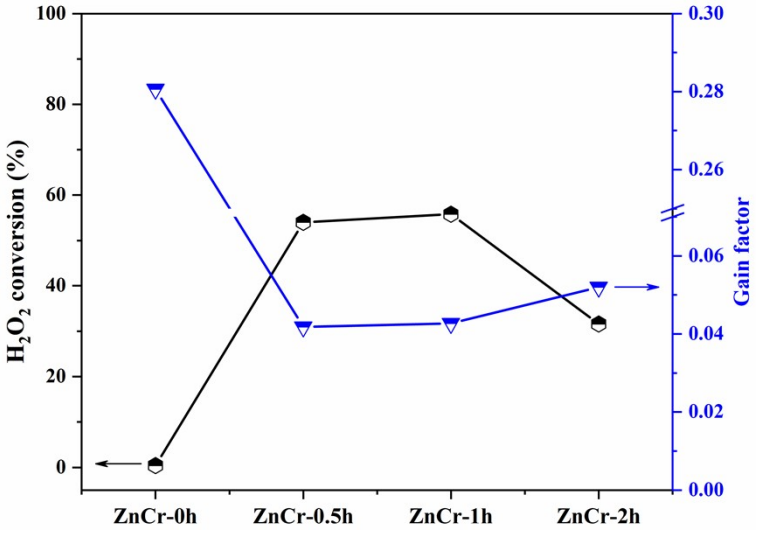

Fig. S13. The H_2O_2 conversion and gain factor over ZnCr-xh.

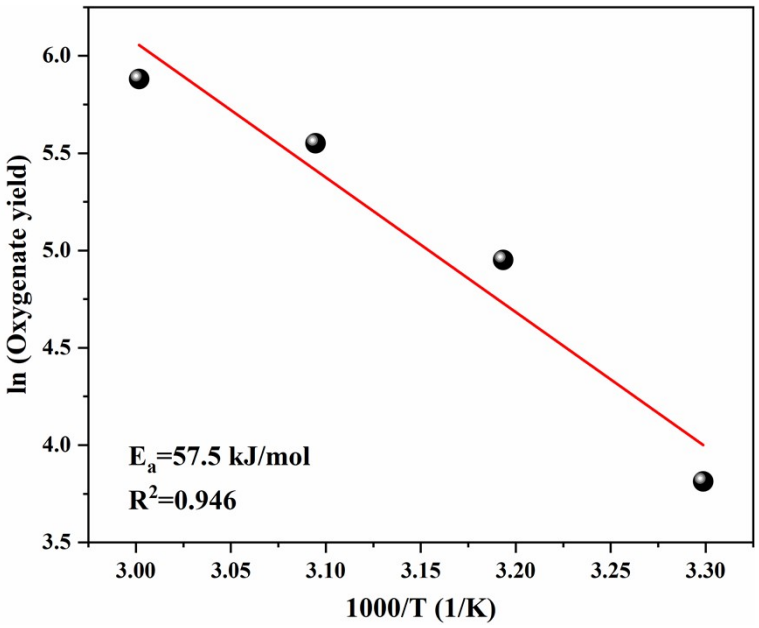

Fig. S14. Arrhenius plots of ZnCr-1h with the temperature ranging from 30 to 60 °C.

Table S3. The compared catalytic performance of various catalysts.

Catalyst	Reactants	T (^{o}C)	Liquid oxygenates		Ref.
			Yield rate (μmol g_{cat}^{-1} h^{-1})	Selectivity (%)	
ZnCr-1h	0.19 M H_2O_2	50	23341 (20 bar CH_4)	90.5	This work
			30695 (30 bar CH_4)	91.4	
Cr_1/TiO_2	3 Mpa CH_4 0.49 M H_2O_2	50	4390	100	[3]
Cu_1/ZSM-5	30 bar CH_4 0.51 M H_2O_2	50	9600	99	[4]
		70	24000	96	
CuO-Pd_1/ZSM-5	30 bar CH_4 5 mM H_2O_2	95	7882	86.5	[5]
FeN_4/GN	1.8 Mpa CH_4 4.90 M H_2O_2	25	228	93.7	[6]
UiO-66-H	3 Mpa CH_4 0.25 M H_2O_2	50	364	100	[7]
AuPd colloid	30 bar CH_4 0.10 M H_2O_2	50	536	94.7	[8]
FeO_x/TiO_2	70 μmol CH_4 8 μmol H_2O_2	light	379.4	97	[9]
ZnO nanosheets	1 bar CH_4 0.49M H_2O_2	light	2210	90.7	[10]
Pd_1/2DT	20 bar CH_4 0.10 M H_2O_2	light	46.3	100	[11]
UiO-66 (2.5TFA)-Fe	3 MPa CH_4 0.29 M H_2O_2	50	4799.2	97.9	[12]
$AuPd/TiO_2$	30.5 bar CH_4 0.5 M H_2O_2	90	1646	88.4	[13]
AuPd@ZSM-5-C16	3 MPa 3.3% H_2/ 6.6 % O_2/1.6 % CH_4/ 61.7 % Ar/26.8 % He	70	4985	100	[14]
Pd_9Au_1 NWs	3 MPa 1.1% H_2/ 2.2% O_2/67.2% CH_4/ 20.6 % Ar/8.9 % He	70	2890.3	99	[15]
PdCu/Z-5	2.4 MPa CH_4 0.3 MPa O_2 0.8 MPa H_2	120	1649.2	95	[16]
Rh_1/ZrO_2	30 bar 95% CH_4/ 5% He 0.5 M H_2O_2	70	76	78.4	[17]
Rh_1/CeO_2	0.5 MPa CH_4 1 M H_2O_2	50	3571.9	93.9	[18]

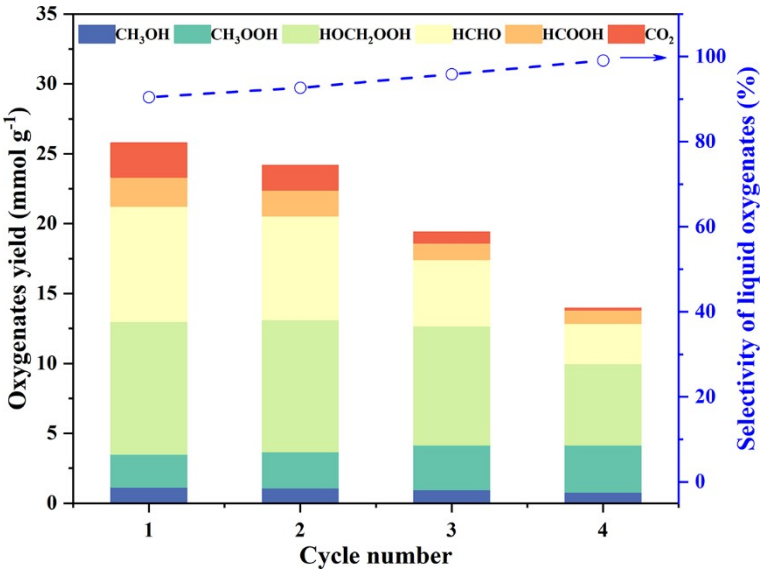

Fig. S15. The product yield and liquid oxygenate selectivity for CH_4 oxidation over ZnCr-1h with four consecutive reaction cycles. The ZnCr-1h catalyst after reaction was collected by centrifugation and redispersed in the fresh reaction solution to perform a new cycle with other reaction conditions unchanged.

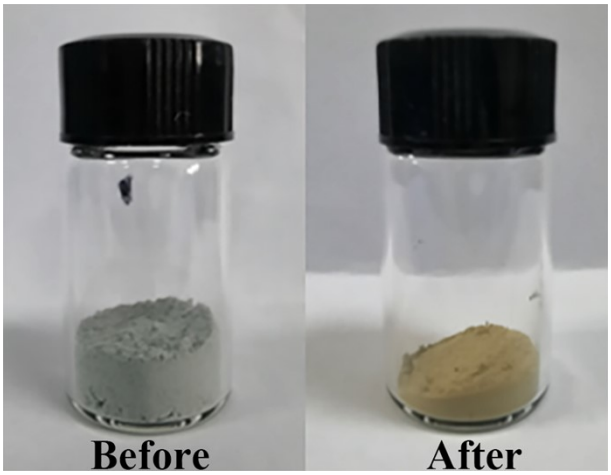

Fig. S16. Digital image of ZnCr-1h nanosheets before and after reaction.

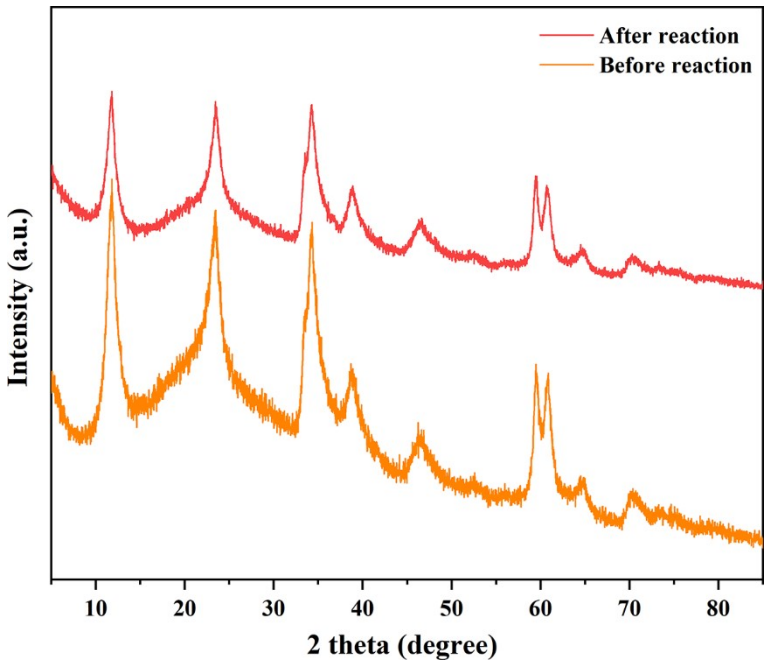

Fig. S17. XRD patterns of ZnCr-1h nanosheets before and after reaction.

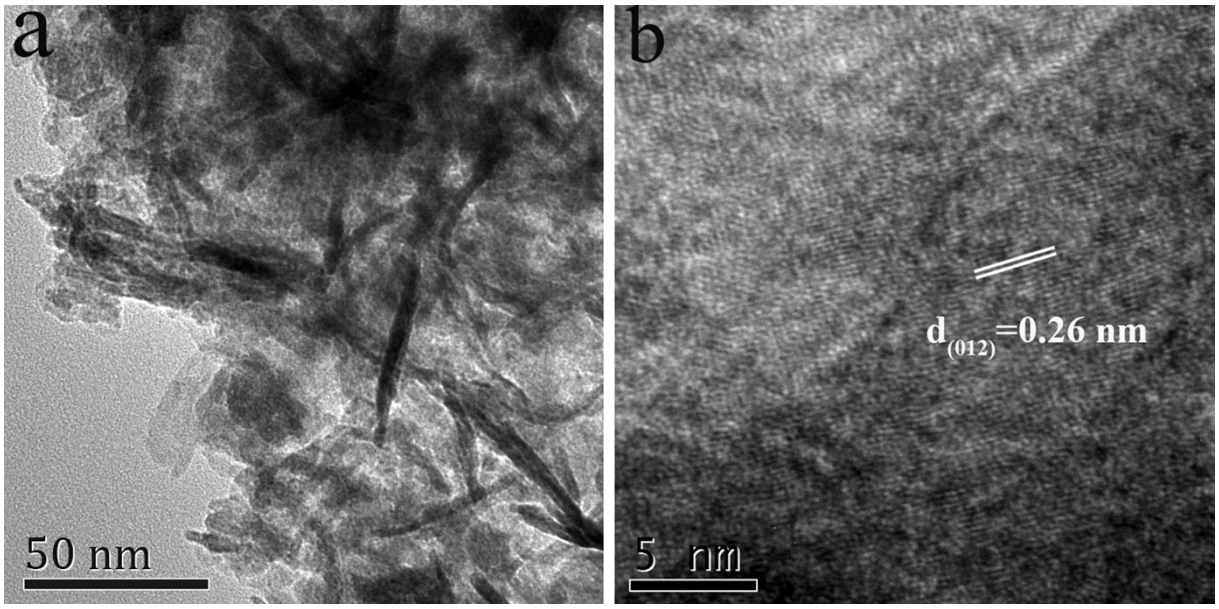

Fig. S18. (a) TEM and (b)HRTEM images of ZnCr-1h nanosheets after reaction.

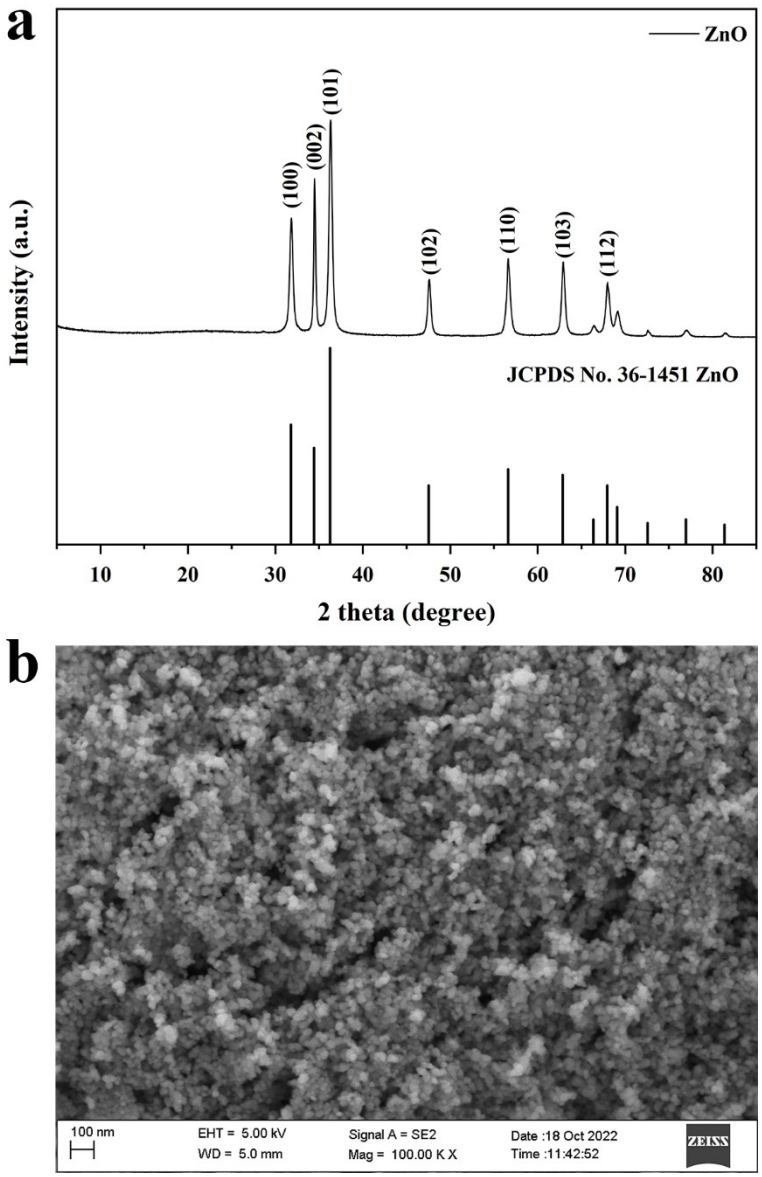

Fig. S19. (a) XRD pattern and (b) SEM image of ZnO nanoparticles.

$Cr^{III} + 3H_2O_2 \rightarrow Cr^{VI} + 3{\cdot}OH + 3OH^-$ .....(1)

$Cr^{VI} + 3H_2O_2 \rightarrow Cr^{III} + 3{\cdot}OOH + 3H^+$ .....(2)

$CH_4 + {\cdot}OH \rightarrow {\cdot}CH_3$ .....(3)

${\cdot}CH_3 + {\cdot}OOH \rightarrow CH_3OOH$; ${\cdot}CH_3 + {\cdot}OH \rightarrow CH_3OH$ .....(4)

$CH_3OH + {\cdot}OH \rightarrow {\cdot}CH_2OH$ .....(5)

${\cdot}CH_2OH + {\cdot}OOH \rightarrow HOCH_2OOH$; ${\cdot}CH_2OH + {\cdot}OH \rightarrow HCHO$ .....(6)

$HCHO + {\cdot}OH \rightarrow {\cdot}CHO$ .....(7)

${\cdot}CHO + {\cdot}OH \rightarrow HCOOH$ .....(8)

$HCOOH + {\cdot}OH \rightarrow CO_2$ .....(9)

Fig. S20. Reaction equations of the consecutive pathway for CH_4 oxidation over etched ZnCr-LDH nanosheets in the presence of H_2O_2.

Table S4. The data collection for the methane oxidation over ZnCr-xh (x = 0, 0.5, 1 and 2) nanosheets.

Catalyst	Entry	Amount of oxygenates (μmol)						Liquid oxygenates (μmol g^{-1})	Liquid oxygenates Selectivity (%)
		CH_3OH	CH_3OOH	$HOCH_2OOH$	HCHO	HCOOH	CO_2		
	1	0.80	8.91	2.19	0	0	5.40	1190	68.8
ZnCr-0h	2	0.64	8.16	1.94	0	0	5.23	1074	67.3
	3	0.58	8.11	1.64	0	0	4.20	1033	71.1
	AVG	0.67	8.39	1.92	0	0	4.94	1099	69.0
	4	12.04	23.78	96.04	73.86	18.07	30.09	22379	88.1
ZnCr-0.5h	5	12.90	24.71	93.37	77.91	16.64	25.32	22553	89.9
	6	9.38	20.30	88.24	79.38	16.57	22.84	21387	90.4
	AVG	11.44	22.93	92.55	77.05	17.09	26.08	22106	89.5
	7	12.04	23.47	86.73	76.44	19.53	25.23	21821	89.6
ZnCr-1h	8	9.60	22.99	96.46	76.81	19.67	21.53	22553	91.3
	9	13.33	24.13	101.82	93.74	23.47	26.25	25649	90.7
	AVG	11.66	23.53	95.00	82.33	20.89	24.34	23341	90.5
	10	9.69	36.34	69.60	38.51	12.14	13.92	16628	92.3
ZnCr-2h	11	6.81	32.56	65.93	38.70	9.93	12.41	15393	92.5
	12	9.34	35.70	74.51	32.99	12.20	9.06	16474	94.8
	AVG	8.61	34.87	70.01	36.73	11.42	11.80	16165	93.2

Table S5. The data collection for the methane oxidation over ZnCr-1h with different methane pressure.

Methane pressure (bar)	Entry	Amount of oxygenates (μmol)						Liquid oxygenates (μmol g^{-1})	Liquid oxygenates Selectivity (%)
		CH_3OH	CH_3OOH	$HOCH_2OOH$	HCHO	HCOOH	CO_2		
0	1	0	0	0	0	0	0	0	0
	2	4.86	19.52	57.61	31.70	11.11	7.74	12480	94.2
10	3	4.64	17.76	47.29	28.57	8.12	6.62	10638	94.1
	4	5.27	19.51	53.35	26.92	8.42	7.25	11347	94.0
	AVG	4.92	18.93	52.75	29.06	9.22	7.20	11488	94.1
	5	12.04	23.47	86.73	76.44	19.53	25.23	21821	89.6
20	6	9.60	22.99	96.46	76.81	19.67	21.53	22553	91.3
	7	13.33	24.13	101.82	93.74	23.47	26.25	25649	90.7
	AVG	11.66	23.53	95.00	82.33	20.89	24.34	23341	90.5
	8	17.83	31.22	114.52	110.00	23.22	33.93	29679	89.7
30	9	16.35	32.81	136.66	102.95	26.91	26.39	31568	92.3
	10	14.35	31.31	147.69	86.75	28.27	26.09	30837	92.2
	AVG	16.18	31.78	132.96	99.90	26.13	28.80	30695	91.4

Table S6. The data collection for the methane oxidation over ZnCr-1h with different amount of H_2O_2.

Amount of H_2O_2 (mL)	Entry	Amount of oxygenates (μmol)						Liquid oxygenates (μmol g^{-1})	Liquid oxygenates Selectivity (%)
		CH_3OH	CH_3OOH	$HOCH_2OOH$	HCHO	HCOOH	CO_2		
0	1	0	0	0	0	0	0	0	0
	2	5.72	15.34	29.74	21.00	4.57	4.29	7637	94.7
0.5	3	5.20	14.25	28.99	16.79	4.89	3.99	7012	94.6
	4	6.07	16.81	36.27	19.36	5.67	4.00	8418	95.5
	AVG	5.66	15.47	31.67	19.05	5.04	4.09	7689	94.9
	5	12.04	23.47	86.73	76.44	19.53	25.23	21821	89.6
1	6	9.60	22.99	96.46	76.81	19.67	21.53	22553	91.3
	7	13.33	24.13	101.82	93.74	23.47	26.25	25649	90.7
	AVG	11.66	23.53	95.00	82.33	20.89	24.34	23341	90.5
	8	11.71	23.45	139.36	120.07	25.79	91.70	32038	77.7
2	9	11.92	22.91	131.54	117.30	25.07	96.74	30874	76.1
	10	13.16	27.02	145.54	100.37	30.62	98.38	31671	76.3
	AVG	12.26	24.46	138.81	112.58	27.16	95.61	31528	76.7

Table S7. The data collection for the methane oxidation over ZnCr-1h with different temperature.

Temp (°C)	Entry	Amount of oxygenates (μmol)						Liquid oxygenates (μmol g^{-1})	Liquid oxygenates Selectivity (%)
		CH_3OH	CH_3OOH	$HOCH_2OOH$	HCHO	HCOOH	CO_2		
	1	4.06	16.03	18.08	4.64	3.26	0.52	4607	98.9
30	2	3.66	11.82	26.84	5.03	4.36	1.51	5171	97.2
	3	2.58	11.33	16.09	3.32	2.50	0.42	3582	98.8
	AVG	3.43	13.06	20.34	4.33	3.37	0.82	4453	98.3
	4	10.28	26.78	61.38	35.38	10.47	2.62	14429	98.2
40	5	9.31	27.56	61.55	28.20	8.52	2.77	13514	98.0
	6	8.52	28.81	64.62	20.29	10.51	6.89	13275	95.1
	AVG	9.37	27.72	62.52	27.96	9.83	4.09	13739	97.1
	7	12.04	23.47	86.73	76.44	19.53	25.23	21821	89.6
50	8	9.60	22.99	96.46	76.81	19.67	21.53	22553	91.3
	9	13.33	24.13	101.82	93.74	23.47	26.25	25649	90.7
	AVG	11.66	23.53	95.00	82.33	20.89	24.34	23341	90.5
	10	12.54	16.47	57.51	111.05	25.32	129.84	22289	63.2
60	11	13.82	19.10	77.07	121.54	27.99	115.82	25952	69.1
	12	12.13	16.52	61.74	106.44	30.24	120.31	22707	65.4
	AVG	12.83	17.36	65.44	113.01	27.85	121.99	23649	65.9

Table S8. The data collection for the methane oxidation over ZnCr-1h with different reaction time.

Reaction time (h)	Entry	Amount of oxygenates (μmol)						Liquid oxygenates (μmol g^{-1})	Liquid oxygenates Selectivity (%)
		CH_3OH	CH_3OOH	$HOCH_2OOH$	HCHO	HCOOH	CO_2		
0.5	1	6.76	26.15	44.63	19.18	8.27	9.13	10499	92.0
	2	5.25	24.77	66.77	21.58	10.13	6.57	12850	95.1
	3	6.71	25.43	72.44	26.73	11.63	8.47	14294	94.4
	AVG	6.24	25.45	61.28	22.50	10.01	8.06	12548	94.0
1	4	12.04	23.47	86.73	76.44	19.53	25.23	21821	89.6
	5	9.60	22.99	96.46	76.81	19.67	21.53	22553	91.3
	6	13.33	24.13	101.82	93.74	23.47	26.25	25649	90.7
	AVG	11.66	23.53	95.00	82.33	20.89	24.34	23341	90.5
2	7	14.15	16.14	53.91	103.32	29.56	135.96	21708	61.5
	8	12.96	15.38	53.17	100.55	27.59	134.17	20965	61.0
	9	15.18	18.76	61.05	109.39	31.42	135.19	23580	63.6
	AVG	14.10	16.76	56.04	104.42	29.52	135.11	22084	62.0

Reference

1. P. Bisgaard, L. MØlhave, B. Rietz and P. Wilhardt, *Anal. Lett.*, 1983, **16**, 1457-1468.
2. F. F. Zhang, Y. L. Zhu, C. Tang, Y. Chen, B. B. Qian, Z. W. Hu, Y. C. Chang, C. W. Pao, Q. Lin, S. A. Kazemi, Y. Wang, L. Zhang, X. W. Zhang and H. T. Wang, *Adv. Funct. Mater.*, 2022, **32**, 2110224.
3. Q. K. Shen, C. Y. Cao, R. K. Huang, L. Zhu, X. Zhou, Q. H. Zhang, L. Gu and W. G. Song, *Angew. Chem., Int. Ed.*, 2020, **59**, 1216-1219.
4. X. Tang, L. Wang, B. Yang, C. Fei, T. Y. Yao, W. Liu, Y. Lou, Q. G. Dai, Y. F. Cai, X. M. Cao, W. C. Zhan, Y. L. Guo, X. Q. Gong and Y. Guo, *Appl. Catal., B*, 2021, **285**, 119827.
5. W. X. Huang, S. R. Zhang, Y. Tang, Y. T. Li, L. Nguyen, Y. Y. Li, J. J. Shan, D. Q. Xiao, R. Gagne, A. I. Frenkel and F. Tao, *Angew. Chem., Int. Ed.*, 2016, **55**, 13441-13445.
6. X. J. Cui, H. B. Li, Y. Wang, Y. L. Hu, L. Hua, H. Y. Li, X. W. Han, Q. F. Liu, F. Yang, L. M. He, X. Q. Chen, Q. Y. Li, J. P. Xiao, D. H. Deng and X. H. Bao, *Chem*, 2018, **4**, 1902-1910.
7. G. Q. Fang, J. N. Hu, L. C. Tian, J. X. Liang, J. Lin, L. Li, C. Zhu and X. D. Wang, *Angew. Chem., Int. Ed.*, 2022, **61**, e202205077.
8. N. Agarwal, S. J. Freakley, R. U. McVicker, S. M. Althahban, N. Dimitratos, Q. He, D. J. Morgan, R. L. Jenkins, D. J. Willock, S. H. Taylor, C. J. Kiely and G. J. Hutchings, *Science*, 2017, **358**, 223-227.
9. J. J. Xie, R. X. Jin, A. Li, Y. P. Bi, Q. S. Ruan, Y. C. Deng, Y. J. Zhang, S. Y. Yao, G. Sankar, D. Ma and J. W. Tang, *Nat. Catal.*, 2018, **1**, 889-896.
10. S. Zhu, X. D. Li, Z. K. Pan, X. C. Jiao, K. Zheng, L. Li, W. W. Shao, X. L. Zu, J. Hu, J. F. Zhu, Y. F. Sun and Y. Xie, *Nano Lett.*, 2021, **21**, 4122-4128.
11. X. Y. Wu, Q. Zhang, W. F. Li, B. T. Qiao, D. Ma and S. L. Wang, *ACS Catal.*, 2021, **11**, 14038-14046.
12. W. S. Zhao, Y. N. Shi, Y. H. Jiang, X. F. Zhang, C. Long, P. F. An, Y. F. Zhu, S. X. Shao, Z. Yan, G. D. Li and Z. Y. Tang, *Angew. Chem., Int. Ed.*, 2021, **60**, 5811-5815.
13. M. H. Ab Rahim, M. M. Forde, R. L. Jenkins, C. Hammond, Q. He, N. Dimitratos, J. A. Lopez-Sanchez, A. F. Carley, S. H. Taylor, D. J. Willock, D. M. Murphy, C. J. Kiely and G. J. Hutchings, *Angew. Chem., Int. Ed.*, 2013, **52**, 1280-1284.
14. Z. Jin, L. Wang, E. Zuidema, K. Mondal, M. Zhang, J. Zhang, C. T. Wang, X. J. Meng, H. Q. Yang, C. Mesters and F. S. Xiao, *Science*, 2020, **367**, 193-197.
15. Y. S. Xu, D. X. Wu, P. L. Deng, J. Li, J. M. Luo, Q. Chen, W. Huang, C. M. Shim, C. M. Jia, Z. X. Liu, Y. J. Shen and X. L. Tian, *Appl. Catal., B*, 2022, **308**, 121223.
16. B. Wu, T. J. Lin, M. Huang, S. G. Li, J. Li, X. Yu, R. O. Yang, F. F. Sun, Z. Jiang, Y. H. Sun and L. S. Zhong, *Angew. Chem., Int. Ed.*, 2022, **61**, e202204116.
17. Y. Kwon, T. Y. Kim, G. Kwon, J. Yi and H. Lee, *J. Am. Chem. Soc.*, 2017, **139**, 17694-17699.

18. S. X. Bai, F. F. Liu, B. L. Huang, F. Li, H. P. Lin, T. Wu, M. Z. Sun, J. B. Wu, Q. Shao, Y. Xu and X. Q. Huang, *Nat. Commun.*, 2020, **11**, 954.